

DISCRETE VORTEX MODELLING OF THE WAKE OF A FLAT PLATE

by

PARAG KUMAR

AE
1993
M
KUM
DIS



**DEPARTMENT OF AEROSPACE ENGINEERING
INDIAN INSTITUTE OF TECHNOLOGY KANPUR**

MAY 1993

DISCRETE VORTEX MODELLING OF THE WAKE OF A FLAT PLATE

A Thesis Submitted
in Partial Fulfilment of the Requirements
for the Degree of

MASTER OF TECHNOLOGY

by

PARAG KUMAR

to the

DEPARTMENT OF AEROSPACE ENGINEERING
INDIAN INSTITUTE OF TECHNOLOGY KANPUR




MAY, 1993

CERTIFICATE

10/5/93
P. M. -

It is certified that the work contained in the thesis entitled "DISCRETE VORTEX MODELLING OF THE WAKE OF A FLAT PLATE", by PARAG KUMAR has been carried out under my supervision and that this work has not been submitted elsewhere for a degree


(Dr Vijay Gupta)

Department of Aerospace Engineering
Indian Institute of Technology, Kanpur

8 May, 1993

AE - 1993 - M - KUM - DIS

- 2 DEC 1993 / AE

CE LIBRARY
CANPUR

Acc No A. 16753

ABSTRACT

The separated flow past a flat plate at an angle of attack has been modelled using the vortex-cloud method. The locations of the nascent vortices have been determined by applying a simplified Kutta condition at the edges of the plate. The strengths of the nascent vortices have been obtained by taking the average shear-layer velocity as determined from the velocities of convection of the first four vortices near the plate. This permits a feedback from the wake to the separation process. The calculated flow features are compared with the reported numerical results and with experiments.

ACKNOWLEDGEMENTS

I take this opportunity to gratefully acknowledge my heartfelt indebtedness to my guide Dr Vijay Gupta Prof in Department of Aerospace Engineering under whose expert supervision this work has been completed. It is only because of his painstaking efforts, kind attitude and constant encouragement that I could carry through the ordeal.

I am indebted to Dr T K Sengupta Asstt Prof in the Department of Aerospace Engineering for his positive suggestions, affectionate attitude and the cooperation he rendered to me from time to time.

I gratefully acknowledge the help and support extended to me by my friends Manoj T Nair and Atul Rathore in the computational work. They were always willing to help me in the hours of need.

I would like to take this opportunity to express my deep sense of gratitude to Mr J K Tyagi, Additional Director ADRDE Agra who has always motivated me for higher studies.

I will fail in my duty if I do not express my appreciation to my wife Babita who gave me great affection, inspiration and support.

(PARAG KUMAR)

*Dedicated
to
My Parents
Wife
and
Dearest Son*

TABLE OF CONTENTS

	Title	Page No
	LIST OF FIGURES	vii
	NOMENCLATURE	viii
Chapter 1	INTRODUCTION	1
1.1	Discrete Vortex Methods	1
1.2	Vortex Cloud Approach	4
1.3	Vortex-in-Cell or Cloud-in-Cell Methods	7
Chapter 2	FORMULATION	10
2.1	The Problem	10
2.2	Mathematical Description	11
2.2.1	Complex Potential and the Transformation used	11
2.2.2	Nascent Vortices and the Kutta Condition	14
2.2.3	Velocities in the Circle and Plate Planes	16
2.3	Method of Calculation	17
2.3.1	Vorticity	17
2.3.2	Introduction and Convection of Vortices	19
2.3.3	Removal and Coalescence of Vortices	24
Chapter 3	RESULTS AND DISCUSSION	26
3.1	Case I. Plate Normal to the Flow	26
3.1.1	Time-Step $t = 0.04$	26
3.1.2	Time-Step $t = 0.03$	37
3.2	Case II. Plate Inclined at 85° to the Flow	37
3.3	Case III. Plate Inclined at 60° to the Flow	44
Chapter 4	CONCLUSIONS	49
Chapter 5	REFERENCES	51

LIST OF FIGURES

- Figure 1. Development of von Karman vortex street from sinusoidally perturbed vortex sheet pair. (Abernathy and Kronauer, 1962)
- Figure 2. Area weighing scheme for the distribution of vorticity on the mesh in Cloud-in-Cell method.
- Figure 3. The wake behind a flat plate at 45° angle of attack at a Reynolds number of 4300. Aluminium flakes suspended in water show its characteristic sinuous form. (Reproduced from Annual Review of Fluid Mechanics, Vol. 13, 1981)
- Figure 4. Flat plate at an angle of attack.
- Figure 5. Flow in the
a) physical (plate) plane;
b) transformed (circle) plane.
- Figure 6. Evolution of wake behind a flat plate. $\alpha = 90^\circ$, $\Delta t = 0.04$.
- Figure 7. Start of asymmetry of wake
a) uniformly accelerated flow around an airfoil at 80° angle of attack;
b) wake flow pattern behind the flat plate during the early stage of flow development computed in the present study.
- Figure 8. Vortex arrangements behind a flat plate. $\alpha = 50^\circ$ (Sarpkaya, 1975)
- Figure 9. Vortex pattern behind a flat plate. $\alpha = 60^\circ$. (Kiya and Arie, 1977)
- Figure 10. Evolution of wake behind a flat plate. $\alpha = 90^\circ$, $\Delta t = 0.03$.
- Figure 11. Vortex shedding pattern behind an inclined flat plate. $\alpha = 85^\circ$, $\Delta t = 0.04$.
- Figure 12. Vortex pattern behind an inclined flat plate. $\alpha = 60^\circ$, $\Delta t = 0.04$.
- Figure 13. Vortex pattern behind an inclined flat plate. $\alpha = 60^\circ$, $\Delta t = 0.03$.

NOMENCLATURE

A	Area of the cell in VIC method
c	Quarter-chord of the flat plate or radius of the circle
f	Frequency of the vortex shedding
h	Cell dimension
i	Imaginary number
p	Counterclockwise (positive) vortex
q	Clockwise (negative) vortex
St	Strouhal number
t	Time
U	Free stream velocity
U_s	Velocity near the separation point
U_{sh}	Velocity in the shear layer
U_{sh_p}	Velocity in the p shear layer
U_{sh_q}	Velocity in the q shear layer
u	x-component of velocity
u_{kp_x}	x-component of velocity of the k^{th} p-vortex
u_{kp_ξ}	ξ -component of velocity of the k^{th} p-vortex
u_{kq_x}	x-component of velocity of the k^{th} q-vortex
u_{kq_ξ}	ξ -component of velocity of the k^{th} q-vortex
V_1	Velocity at the outer edge of the shear layer
V_2	Velocity at the inner edge of the shear layer
v	y-component of velocity
v_{kp_y}	y-component of velocity of the k^{th} p-vortex
v_{kp_η}	η -component of velocity of the k^{th} p-vortex
v_{kq_y}	y-component of velocity of the k^{th} q-vortex
v_{kq_η}	η -component of velocity of the k^{th} q-vortex
w	Complex potential function

z	Point in the physical (plate) plane ($z = x+iy$)
α	Angle of attack
Δt	Time-step
δ	Boundary layer thickness
Γ	Circulation
ω	Vorticity
ψ	Stream function
ζ	Point in the transformed (circle) plane

INTRODUCTION

1.1 Discrete Vortex Methods

The establishment by L. Prandtl in 1903 that fluid flows at large values of Reynolds number can be modelled as essentially inviscid flows with thin regions of viscous activities near the solid boundaries could not be used with profit in flow about bluff bodies, where the separation of these thin regions of viscous flow (termed as boundary layer) from the solid surfaces disturbed the flows rather drastically so that the inviscid methods could not be of much use.

The vortex methods for treating such flows evolved slowly and built upon the concepts introduced by various researchers.

Th. von Karman had shown in 1911 that the wake of a bluff body consisted of a series of vortices shed alternately from the two separation points. Helmholtz has shown earlier in 1938 that in an inviscid flow, vortex lines are material lines, that is, they are continually composed of the same fluid particles and that flows with vorticity can be modelled with 'line vortices' of appropriate circulation and infinitesimal cross-section. It is this realization which led to discretization of compact regions of vorticity into a collection of vortices embedded in an otherwise potential flow.

Rosenhead (1931) appears to be the first person to use this approach to study the Kelvin-Helmholtz instability of vortex sheets. He discretized a vortex sheet into a number of discrete

vortices and allowed these vortices to convect under mutual influence with an initial sinusoidal perturbation to the (x,y) coordinates of the vortices. After a number of time steps vortex roll-ups develop along the sheet at the crest and trough of each sine-wave culminating finally in a single row of vortex bunches (termed as clouds), very similar to half a Karman vortex street. There is a remarkable and dramatic self-convective activity following a small perturbation.

Rosenhead's success with convection of discrete vortices to model vortex sheet had a very seductive influence on later researchers. Abernathy and Kronauer(1962) extended this method to modelling the alternating vortex shedding in the wake of the circular cylinder, a problem of much fascination to researchers since von Karman first analyzed it in 1911. Apart from the initial disturbance(Figure 1) the motion is self-induced entirely by the convective processes of all the interacting discrete vortices. Abernathy and Kronauer concluded from this study that the role of a bluff body is not very important in the formation of its detailed vortex-street wake, excluding its function in the generation of the two separate vortex shear layers responsible for feeding vortex into the wake.

Much of the recent work on discrete vortex modelling has been reviewed by Clements and Maull(1975), Saffman and Baker(1979) and Sarpkaya(1989).

The problem of wake behind bluff bodies has been studied by many researchers. Almost all such studies involve some variation in technique, and all of them rely on some ad-hoc assumption or the other.

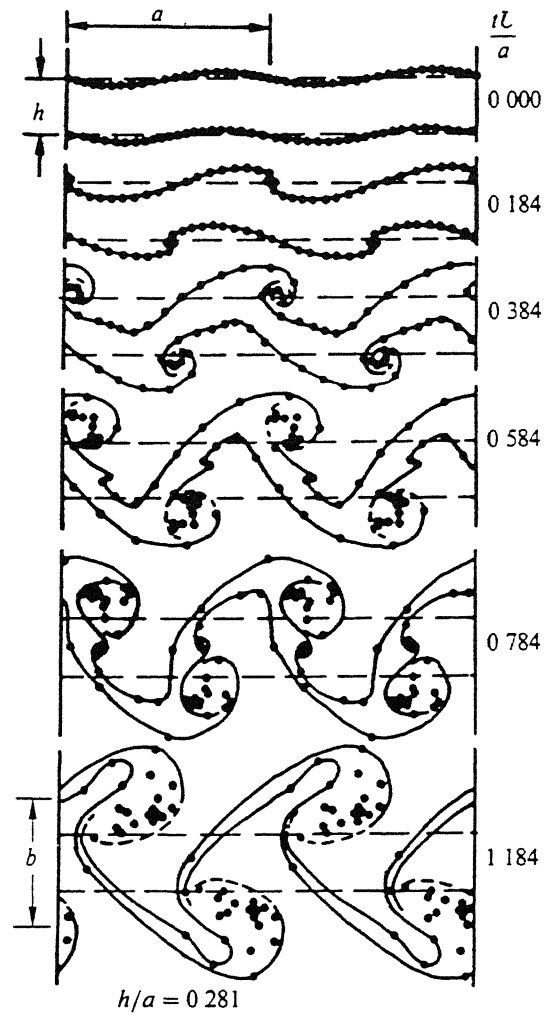


Figure 1 Development of von Karman vortex street from sinusoidally perturbed vortex sheet pair (Abernathy and Kronauer, 1962)

1.2 Vortex-Cloud Approach

The 'classical' approach to the problem has been termed as the vortex cloud approach for the fact that the discretized vortex sheet is now represented by a cloud of discretized point (in 2 - dimensions) vortices. The natural scheme of calculation in such a model follows Lagrangian approach wherein discrete vortices which are natural points following Helmholtz are convected downstream under the combined influence of the inviscid flow and the mutually induced velocity of the various vortices constituting the cloud. A marching-in-time scheme is used. The calculations have a dramatic advantage in that they are grid-independent. The inviscid flow can be modelled using conformal transformation, and so explicit boundary conditions need to be used once the image systems are employed to preserve the streamline shapes at the body.

This basic scheme has been taken through a lot of variations in respect to the manner in which vorticity is introduced continually in flow - in the location of introduction of new vortices (termed as nascent vortices) and the strength of nascent vortices, in the scheme for keeping track of the vortices and in methods of cancellation and coalescence of vortices.

Clements(1973) and Kiya and Arie(1977 1980) prefer the use of fixed nascent vortex positions, where new vortices appear periodically at fixed location close to (but not at) the separation point. The rate of vorticity generation is obtained from the velocity U_s at these points

$$\frac{d\Gamma}{dt} = \frac{1}{2} U_s^2 \quad (11)$$

This formulation is sought to be justified from the pioneering

work of Fage and Johansen(1928) on structure of vortex sheets Kiya and Arie(1977) allowed the variations of these fixed points between subjective limits and compared the calculated results with those obtained experimentally to obtain a proper location of separation point. The effect of the position of the nascent vortices on the velocity distribution in the neighborhood of the separation point was not examined at all.

Sarpkaya(1989) refers to a work of Kuwahara (Numerical study of flow past an inclined flat plate by an inviscid model J Phys Soc , Japan, vol 35, 1545(1973)) wherein the strengths of the nascent point vortices (at fixed locations) are determined from Kutta condition. Kuwahara is reported to have found that the amplitude of the normal force coefficient calculated in this manner depends very strongly upon the assumed position of the two fixed points where the nascent vortices appear. In fact, a small change in the position of nascent vortices is reported to cause an eight-fold change in the normal force coefficient.

Based on these considerations, Sarpkaya(1975) introduced a procedure wherein he used variable nascent vortex positions and determined the rate of shedding of vorticity from the relation

$$\frac{\partial \Gamma}{\partial t} = \frac{1}{2} U_{sh}^2 \quad (12)$$

where U_{sh} is the velocity in the shear layer calculated using the average of the convective velocities of the first four vortices in each shear layer. The location of the appearance of the nascent vortices is determined so as to satisfy the Kutta condition at the edges of the body. This method appears to provide a satisfactory feedback mechanism from wake fluctuations to the rate at which vorticity is shed, a shortcoming of almost all the other methods.

Sarpkaya working with others has extended his method to various other geometries like cambered porous plate which model flow through parachute canopies rectangular prisms and even about oscillating plates(1990, 1986, 1979, 1982)

The survey of literature of the vortex cloud method shows that the method works but only to a limited extent All applications involved the use of a number of adjustable parameters to make the scheme work and the following main difficulties are observed

a) Groups of discrete vortices moving under their mutual influence inevitably lead to a random distribution (Sarpkaya and Shoaff, 1979)

b) Inviscid flow theory does not permit destruction or dissipation of vorticity But in real flows only a fraction (say, about 60%) of the circulation fed into the shear layer is found in vortex clusters (Mair and Maull, 1971) Different ad-hoc modifications are incorporated in models, in violation of the vortex theorems in order to account for the circulation loss brought about by the rear face shear layer, and the viscous and turbulent diffusion

c) The Lagrangian approach adopted in calculation requires a large number of vortices whose velocities due to mutual influence need to be calculated This requires n^2 velocity calculations for every time-step, where n is the number of vortices, with n tending to be very large Some or the other scheme has to be devised to save time Thus, vortex clouds are coalesced somewhat arbitrarily to limit computer time

d) Contrary to practical results, the numerical simulation of symmetrically started flows remain symmetrical for a long time till round-off errors pile up and start an asymmetry. Thus the initial time calculation do not give valid results, and large-time results are vitiated by the difficulty mentioned in (a) above. Consequently only a small window of time, large enough to start the asymmetrical behavior but small enough for the random distribution not having set in, is available for useful results. This precludes meaningful studies of say opening characteristics of parachute canopies.

1.3 Vortex-in-Cell (VIC) or Cloud-in-Cell (CIC) Methods

The calculation of velocities of large number of vortices (as many as 100 000) by adding the mutual influence of all of them stretches the capacity of even the fastest available computer. In line with the hybrid Lagrangian-Eulerian approach of Particle-in-Cell (PIC) or Marker-in-Cell (MIC) (Harlow, 1964) a Cloud-in-Cell or Vortex-in-Cell method has been developed (Birdsall and Fuss (1969), Langdon (1970), Christiansen (1973), Baker (1979), and Smith and Stansby (1988)). These methods combined the best features of both the Lagrangian and the Eulerian approaches. The Lagrangian vortices move through a fixed Eulerian grid.

The method consists of assigning the vorticity of each vortex to the four neighboring grid points in the manner of double interpolation. Thus the vorticity of the n^{th} vortex in a given cell is assigned to the four surrounding mesh points (Figure 2).

according to

$$\omega_i = \Gamma_n A_i / A^2 \quad i = 1, 2, 3, 4 \quad (13)$$

where Γ_n is the circulation of the vortex and A is the area of the cell

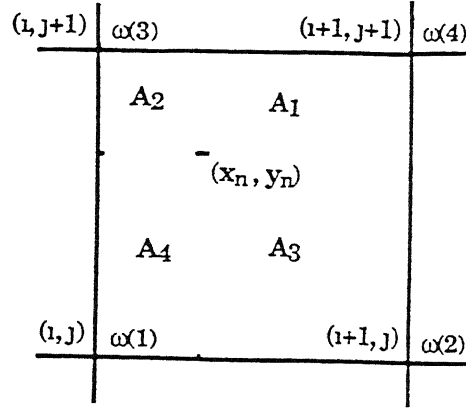


Figure 2. Area weighing scheme for the distribution of vorticity on the mesh in cloud-in-cell method

Once the vorticity of all cells is so allocated, the Poisson equation

$$\nabla^2 \psi = -\omega \quad (14)$$

is solved for the region to obtain $\psi_{i,j}$ for all the mesh points (i, j) . The velocity components are then calculated at each of the mesh points from the given values of ψ through a simple central differencing scheme

$$u_{i,j} = (\psi_{i,j+1} - \psi_{i,j-1}) / 2h \quad (15)$$

$$v_{i,j} = -(\psi_{i+1,j} - \psi_{i-1,j}) / 2h \quad (16)$$

where h is the cell dimension

Once the velocities at the mesh points are obtained, the velocity for each vortex is obtained by double interpolation

$$u_n = \sum u_i A_i / A \quad (17)$$

$$v_n = \sum v_i A_i / A \quad (18)$$

Thus in this hybrid scheme, the Eulerian velocity field is

obtained from which the velocity of each vortex is obtained and then each vortex is convected in a Lagrangian manner.

This method requires less time and enables one to track a large number of vortices. However, Sarpkaya(1989) has pointed out few drawbacks of this method. It makes an otherwise grid-free method once again grid-dependent. The method and its time-scale behavior are sensitive to the size of the mesh, the surface boundary conditions, the number of vortices and the time-step. The flow features of scale smaller than the grid cannot be accurately resolved. Christiansen(1973) on the basis of numerical experiments has found that the most significant numerical error in this scheme arises from the anisotropic CIC - interpolation of velocities.

The present work uses Discrete Vortex Model to simulate inviscid two-dimensional vortex shedding behind a flat plate. It uses the method of variable nascent vortex positions as used by Sarpkaya(1975). Numerical experiments are conducted by taking the angle of inclination of the plate to the flow of 60° , 85° and 90° and using the time steps of 0.03 and 0.04. The following chapters discuss in detail the mathematical description of the model, the algorithm used and the results obtained.

FORMULATION

2.1 The Problem

This investigation is concerned with the use of the Discrete Vortex Method for the study of the separating flow from an inclined flat plate kept in a uniform flow with a free stream velocity U as shown in Figure 3. The nomenclature used is shown in Figure 4.



Figure 3 The wake behind a flat plate at 45° angle of attack at a Reynolds number of 4300. Aluminum flakes suspended in water show its characteristic sinuous form (Reproduced from Annual Review of Fluid Mechanics, Vol 13, 1981)

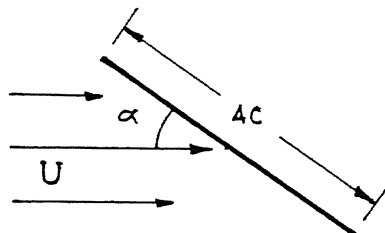


Figure 4 Flat plate at an angle of attack

2.2 Mathematical Description

2.2.1 Complex Potential and the Transformation Used

The approach used consists of transforming the plate plane z into a circle plane using Joukowski transformation. This relates the ζ -plane to z -plane by the relation

$$z = \zeta + \frac{c^2}{\zeta} \quad (2.1)$$

The complex potential for flow in the circle plane at an angle α as shown in Figure 5 can be written as

$$w(\zeta) = U \zeta e^{-i\alpha} + \frac{U c^2 e^{i\alpha}}{\zeta} \quad (2.2)$$

where c is the quarter-chord of the flat plate or the radius of the circle in the ζ -plane

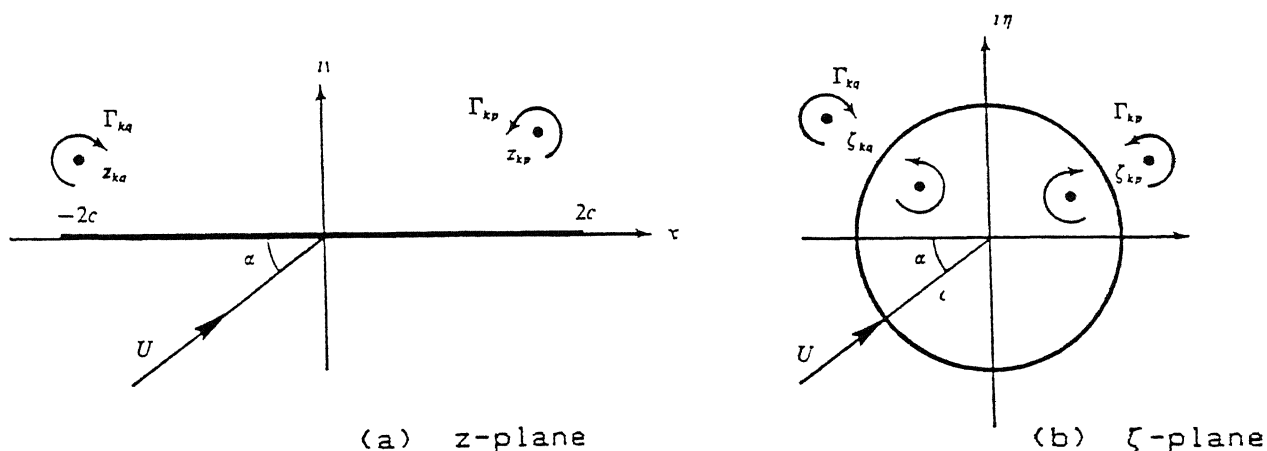


Figure 5. Flow in the (a) physical (plate) plane, and (b) transformed (circle) plane

This represents a non-separate flow past the circle (or flat plate in the z -plane) To simulate the vortex sheet of the separated flow, we add a series of discrete point vortices in the flow Let us use the following nomenclature Let Γ_{kp} represent the strength of the counterclockwise k^{th} vortex shed from the trailing edge ($x = + 2c$) of the flat plate in the z -plane and Γ_{kq} the strength of the clockwise k^{th} vortex shed from the leading edge ($x = - 2c$) We differentiate between the two series for ease in coding including the fact that with this approach we can take both Γ_{kp} and Γ_{kq} to be positive throughout

The complex potential for a p -vortex, therefore is

$$+ \frac{\Gamma_{kp}}{2\pi} \ln (\zeta - \zeta_{kp})$$

and that for a q -vortex is

$$- \frac{\Gamma_{kq}}{2\pi} \ln (\zeta - \zeta_{kq})$$

But these potentials can not be added directly to that of flow past a circle, since it would change the shape of the stagnation streamline which would no longer satisfy the boundary condition of the flow

For this purpose, we use the circle theorem For a vortex of strength $\Gamma/2\pi$ at a point $\zeta' = \xi' + i \eta'$ outside the circle $|\zeta|=c$, the circle theorem gives the complex potential as

$$w(\zeta) = + \frac{\Gamma}{2\pi} \ln (\zeta - \zeta') - \frac{\Gamma}{2\pi} \ln (\zeta - \frac{c^2}{\bar{\zeta}'}) + \frac{\Gamma}{2\pi} \ln \zeta \quad (2.3)$$

where the first term on the right represents the potential of the vortex situated at ζ' and the second term that of the image of

this vortex located at the inverse point and having a strength $-\Gamma/2\pi$ (Milne-Thomson, 1969)

The last term represents the image at the centre. But in the present case, there are no images at the centre of the cylinder because the vortices have been shed from the cylinder and leave circulation opposite to their own on the body. This last term is equal and opposite to the circulation due to vortex at the centre and thus cancels it.

Making use of Equation 2.3, the complex potential function w in the circle (ζ) plane (see Figure 5) which describes a uniform flow U with a doublet at the origin to simulate the cylinder, $k+1$ vortices rotating counterclockwise on the right-hand side of the wake (called p-vortices), $k+1$ vortices rotating clockwise on the left-hand side of the wake (called q-vortices), and the images of all the p- and q- vortices in the circle may be written as

$$\begin{aligned}
 w(\zeta) = & -U \left(\zeta e^{-i\alpha} + \frac{c^2}{\zeta} e^{i\alpha} \right) + i \frac{\Gamma_{op}}{2\pi} \ln(\zeta - \zeta_{op}) \\
 & - i \frac{\Gamma_{op}}{2\pi} \ln\left(\zeta - \frac{c^2}{\bar{\zeta}_{op}}\right) + \sum_{k=1}^m i \frac{\Gamma_{kp}}{2\pi} \ln(\zeta - \zeta_{kp}) \\
 & - \sum_{k=1}^m i \frac{\Gamma_{kp}}{2\pi} \ln\left(\zeta - \frac{c^2}{\bar{\zeta}_{kp}}\right) - i \frac{\Gamma_{oq}}{2\pi} \ln(\zeta - \zeta_{oq}) \\
 & + i \frac{\Gamma_{oq}}{2\pi} \ln\left(\zeta - \frac{c^2}{\bar{\zeta}_{oq}}\right) - \sum_{k=1}^m i \frac{\Gamma_{kq}}{2\pi} \ln(\zeta - \zeta_{kq}) \\
 & + \sum_{k=1}^m i \frac{\Gamma_{kq}}{2\pi} \ln\left(\zeta - \frac{c^2}{\bar{\zeta}_{kq}}\right) \quad (2.4)
 \end{aligned}$$

in which Γ_{kp} and ζ_{kp} represent respectively the strength and

location of the k^{th} p-vortex, Γ_{kq} and ζ_{kq} the strength and location of the k^{th} q-vortex, and c the radius of the cylinder an overbar indicates a complex conjugate

2.2.2 Nascent Vortices and the Kutta Condition

Γ_{op} and Γ_{oq} located at ζ_{op} and ζ_{oq} respectively are called the 'nascent vortices' or 'Kutta vortices' These represent the first vortices introduced into the flow at each edge of the plate The positions of these nascent vortices are chosen so as to satisfy the Kutta condition at each edge of the plate In accordance with this condition, the flow separates tangentially at the edges of the plate Thus,

$$dw/d\zeta = 0 \quad \text{at} \quad \zeta = \pm c \quad (25)$$

in the circle plane and dw/dz gives a finite velocity at $z = \pm 2c$ in the plate plane Inserting Equation 2.4 in 2.5, we get two equations

$$\begin{aligned} & -U(e^{-i\alpha} - e^{i\alpha}) + i \frac{\Gamma_{op}}{2\pi} \frac{1}{c - \zeta_{op}} - i \frac{\Gamma_{op}}{2\pi} \frac{1}{c - c^2/\bar{\zeta}_{op}} \\ & + \sum_{k=1}^m i \frac{\Gamma_{kp}}{2\pi} \frac{1}{c - \zeta_{kp}} - \sum_{k=1}^m i \frac{\Gamma_{kp}}{2\pi} \frac{1}{c - c^2/\bar{\zeta}_{kp}} - i \frac{\Gamma_{oq}}{2\pi} \frac{1}{c - \zeta_{oq}} \\ & + i \frac{\Gamma_{oq}}{2\pi} \frac{1}{c - c^2/\bar{\zeta}_{oq}} - \sum_{k=1}^m i \frac{\Gamma_{kq}}{2\pi} \frac{1}{c - \zeta_{kq}} + \sum_{k=1}^m i \frac{\Gamma_{kq}}{2\pi} \frac{1}{c - c^2/\bar{\zeta}_{kq}} = 0 \end{aligned} \quad (26)$$

$$\begin{aligned}
& -U(e^{-i\alpha} - e^{i\alpha}) - i \frac{\Gamma_{op}}{2\pi} \frac{1}{c + \zeta_{op}} + i \frac{\Gamma_{op}}{2\pi} \frac{1}{c + c^2/\bar{\zeta}_{op}} \\
& - \sum_{k=1}^m i \frac{\Gamma_{kp}}{2\pi} \frac{1}{c + \zeta_{kp}} + \sum_{k=1}^m i \frac{\Gamma_{kp}}{2\pi} \frac{1}{c + c^2/\bar{\zeta}_{kp}} + i \frac{\Gamma_{oq}}{2\pi} \frac{1}{c + \zeta_{oq}} \\
& - i \frac{\Gamma_{oq}}{2\pi} \frac{1}{c + c^2/\bar{\zeta}_{oq}} + \sum_{k=1}^m i \frac{\Gamma_{kq}}{2\pi} \frac{1}{c + \zeta_{kq}} - \sum_{k=1}^m i \frac{\Gamma_{kq}}{2\pi} \frac{1}{c + c^2/\bar{\zeta}_{kq}} = 0
\end{aligned} \tag{2.7}$$

Equations 2.6 and 2.7 are solved to get the positions of the two nascent vortices. While solving these equations, two assumptions are made for simplification

(i) The vortices Γ_{op} and Γ_{oq} are introduced along the ξ -axis, i.e.,

$$\eta_{op} = \eta_{oq} = 0 \tag{2.8}$$

(ii) The effect of Γ_{op} and Γ_{oq} on each other at the time of introduction is negligible

Thus in Equation 2.6, we neglect the term containing Γ_{oq} and similarly in 2.7, the term containing Γ_{op}

Simplifying the two equations with the above considerations we get the positions as

$$\zeta_{op} = \frac{\frac{c^2 c_1}{\Gamma_{op}/2\pi} - c}{1 + \frac{c c_1}{\Gamma_{op}/2\pi}} \tag{2.9}$$

and

$$\zeta_{oq} = \frac{c - \frac{c^2 c_2}{\Gamma_{oq}/2\pi}}{1 + \frac{c c_2}{\Gamma_{oq}/2\pi}} \tag{2.10}$$

where

$$c_1 = -2U \sin \alpha - \sum_{k=1}^m \frac{\Gamma_{kp}}{2\pi} \left[\frac{c + \xi_{kp}}{c (c - \xi_{kp})} \right] + \sum_{k=1}^m \frac{\Gamma_{kq}}{2\pi} \left[\frac{c + \xi_{kq}}{c (c - \xi_{kq})} \right] \quad (2.11)$$

$$c_2 = -2U \sin \alpha + \sum_{k=1}^m \frac{\Gamma_{kp}}{2\pi} \left[\frac{c - \xi_{kp}}{c (c + \xi_{kp})} \right] - \sum_{k=1}^m \frac{\Gamma_{kq}}{2\pi} \left[\frac{c - \xi_{kq}}{c (c + \xi_{kq})} \right] \quad (2.12)$$

2.2.3 Velocities in the Circle and Plate Planes

The advancement of the position of each vortex in the z -plane at the end of each time interval requires the transformation of the positions of all vortices into the circle plane, the calculation of the velocities at each vortex center in the circle plane and, finally the reverse transformation of the velocities from the circle to the plate plane

For calculating the velocity components in the circle plane of any vortex the k^{th} , say, the complex potential of that vortex is subtracted from the total potential given by Equation 2.4 and evaluating the derivative of the remaining terms at $\zeta = \zeta_k$

Using the above procedure, the potentials of the k^{th} p-vortex and the k^{th} q-vortex may be written as

$$w_{kp}(\zeta) = w(\zeta) - i \frac{\Gamma_{kp}}{2\pi} \ln(\zeta - \zeta_{kp}) \quad (2.13)$$

and

$$w_{kq}(\zeta) = w(\zeta) + i \frac{\Gamma_{kq}}{2\pi} \ln(\zeta - \zeta_{kq}) \quad (2.14)$$

The velocities, then, in the ζ -plane are given by

$$-u_{kp\xi} + i v_{kp\eta} = \left[dw_{kp}(\zeta) / d\zeta \right]_{\zeta = \zeta_{kp}} \quad (2.15)$$

and

$$-u_{kq\xi} + i v_{kq\eta} = \left[dw_{kq}(\zeta) / d\zeta \right]_{\zeta = \zeta_{kq}} \quad (2.16)$$

The velocities in the plate plane are then calculated using the relations

$$-u_{kp_x} + i v_{kp_y} = (-u_{kp\xi} + i v_{kp\eta}) \frac{\zeta_{kp}^2}{\zeta_{kp}^2 - c^2} - i \frac{\Gamma_{kp}}{2\pi} \frac{\zeta_{kp} c^2}{(\zeta_{kp}^2 - c^2)^2} \quad (2.17)$$

$$-u_{kq_x} + i v_{kq_y} = (-u_{kq\xi} + i v_{kq\eta}) \frac{\zeta_{kq}^2}{\zeta_{kq}^2 - c^2} - i \frac{\Gamma_{kq}}{2\pi} \frac{\zeta_{kq} c^2}{(\zeta_{kq}^2 - c^2)^2} \quad (2.18)$$

which are derived using the transformation

2.3 Method of Calculation

2.3.1 Vorticity

The rate of shed of vorticity into the wake is given by

$$\int_0^{\delta} \left(\frac{\partial v}{\partial x} - \frac{\partial u}{\partial y} \right) u \, dy \quad (2.19)$$

where δ is the boundary layer thickness. This may be approximated by

$$\frac{\partial \Gamma}{\partial t} = \frac{1}{2} (V_1^2 - V_2^2) \quad (2.20)$$

where V_1 and V_2 represent the velocities at the outer and inner edges of the shear layer

Fage and Johansen (1928), on the basis of experiments with various bluff bodies have shown that vorticity is shed from the two sides of an asymmetric body at the same rate and that the velocity V_1 at the outer edge of the sheet is much larger than the velocity V_2 at the inner edge. Thus we can ignore the term V_2^2 in the above expression for vorticity flux to simplify the expression as

$$\frac{\partial \Gamma}{\partial t} \approx \frac{1}{2} V_1^2 \quad (2.21)$$

Now the question comes of selecting the velocity. There has been varied opinion by investigators regarding the selection of a point at which the velocity should be considered for calculating the vorticity flux as also mentioned in chapter 1. Clements (1973) and Clements & Maull (1975) selected a fixed point in the flow near the separation point and used the velocity U_s at that point to calculate the rate of shed of vorticity using Equation 1.1

Kiya and Arie (1980) proposed a 'velocity-point scheme', in which a 'velocity-point' is introduced in front of the plate along a line perpendicular to the plane of the plate and drawn through the edge concerned, which they interpreted as the edge of the boundary layer at the separation points. The velocity U_s at that point was used to determine the strength of the nascent vortices.

Sarpkaya (1975, 1989), however, felt that in these methods no interaction is allowed between the shed vortices and the amplitude of oscillation of the point or the time of appearance of the nascent vortices. He used the velocity U_{sh} in the shear layer for calculating the vorticity flux (Equation 1.2)

It is felt that the various schemes are quite arbitrary. In the present work, Sarpkaya's (1975) approach has been used as it

appears to simulate the mechanism of feedback from wake fluctuations to the fluctuations in the rate of circulation

U_{sh} is calculated by using the average of the transport velocities of the first four vortices in each shear layer. Thus

$$U_{sh_p} = \frac{1}{4} \sum_{k=1}^4 (u_{kp}^2 + v_{kp}^2)^{1/2} \quad (2.22)$$

$$U_{sh_q} = \frac{1}{4} \sum_{k=1}^4 (u_{kq}^2 + v_{kq}^2)^{1/2} \quad (2.23)$$

Sarpkaya(1975) suggests that the use of the velocity at the position of a single vortex (with $k=1$ say) to estimate the shear layer velocity would not be satisfactory partly because Γ_{1p} or Γ_{1q} vortices are too close to the edges of the plate and the radius of curvature of their pathlines are relatively small. Thus the numerical errors involved in the determination of their transport velocities could give rise to unacceptable oscillations in the vorticity flux. The use of the average of the transport velocities of a number of vortices in each shear layer would therefore give a better representation of the velocity and vorticity flux in the shear layers. After several preliminary calculations, he has concluded that taking U_{sh} as the average of the velocities of the first four vortices will be quite satisfactory.

2.3.2 Introduction and Convection of Vortices

The method of introduction, as well as the subsequent convection, of the nascent vortices plays an important role in the evolution of wake by discrete vortex method. They are required to

be introduced at very small time intervals and convected in a manner that they can follow the true streamlines in the regions of flow where the streamlines are rapidly curving

To introduce the first vortex, use is made of the results of Fage and Johansen(1928) who showed that the velocity V_1 in a shear layer in a steady flow is about $1.4U$, where U is the freestream velocity. Thus from Equation 2.21, we get

$$\begin{aligned}\frac{\partial \Gamma}{\partial t} &\cong \frac{1}{2} V_1^2 \\ &\cong \frac{1}{2} (1.4 U)^2 \\ &\cong U^2\end{aligned}\quad (2.24)$$

As the non-dimensional free stream velocity is equal to unity we have

$$\Delta \Gamma \cong \Delta t \quad (2.25)$$

Accordingly, the strengths Γ_{1p} and Γ_{1q} of the first vortices are taken equal to $5 \Delta t$. The positions of Γ_{1p} and Γ_{1q} are found using the Kutta condition Equations 2.6 and 2.7 which are reduced with only the first vortices present in the flow to

$$\begin{aligned}-U(e^{-i\alpha} - e^{i\alpha}) + i \frac{\Gamma_{1p}}{2\pi} \frac{1}{(c - \zeta_{1p})} - i \frac{\Gamma_{1p}}{2\pi} \frac{1}{(c - c^2/\bar{\zeta}_{1p})} \\ - i \frac{\Gamma_{1q}}{2\pi} \frac{1}{(c - \zeta_{1q})} + i \frac{\Gamma_{1q}}{2\pi} \frac{1}{(c - c^2/\bar{\zeta}_{1q})} = 0\end{aligned}\quad (2.26)$$

$$\begin{aligned}-U(e^{-i\alpha} - e^{i\alpha}) - i \frac{\Gamma_{1p}}{2\pi} \frac{1}{(c + \zeta_{1p})} + i \frac{\Gamma_{1p}}{2\pi} \frac{1}{(c + c^2/\bar{\zeta}_{1p})} \\ + i \frac{\Gamma_{1q}}{2\pi} \frac{1}{(c + \zeta_{1q})} - i \frac{\Gamma_{1q}}{2\pi} \frac{1}{(c + c^2/\bar{\zeta}_{1q})} = 0\end{aligned}\quad (2.27)$$

Here an assumption is made that these starting vortices are introduced along the ξ -axis, i.e.,

$$\eta_{1p} = \eta_{1q} = 0 \quad (2.28)$$

This assumption simplifies the equations to a great extent and the ξ -coordinates of the first p- and q- vortices can be found solving the simple algebraic equations

Now, to calculate the velocities of these first vortices, we write the potential for the situation when only Γ_{1p} and Γ_{1q} are present

$$\begin{aligned} w(\zeta) = & -U \left(\zeta e^{-i\alpha} + \frac{c^2}{\zeta} e^{i\alpha} \right) + i \frac{\Gamma_{1p}}{2\pi} \ln(\zeta - \zeta_{1p}) - i \frac{\Gamma_{1p}}{2\pi} \ln\left(\zeta - \frac{c^2}{\bar{\zeta}_{1p}}\right) \\ & - i \frac{\Gamma_{1q}}{2\pi} \ln(\zeta - \zeta_{1q}) + i \frac{\Gamma_{1q}}{2\pi} \ln\left(\zeta - \frac{c^2}{\bar{\zeta}_{1q}}\right) \end{aligned} \quad (2.29)$$

$$\begin{aligned} w_{1p}(\zeta) &= w(\zeta) - i \frac{\Gamma_{1p}}{2\pi} \ln(\zeta - \zeta_{1p}) \\ &= -U \left(\zeta e^{-i\alpha} + \frac{c^2}{\zeta} e^{i\alpha} \right) - i \frac{\Gamma_{1p}}{2\pi} \ln\left(\zeta - \frac{c^2}{\bar{\zeta}_{1p}}\right) \\ &\quad - i \frac{\Gamma_{1q}}{2\pi} \ln(\zeta - \zeta_{1q}) + i \frac{\Gamma_{1q}}{2\pi} \ln\left(\zeta - \frac{c^2}{\bar{\zeta}_{1q}}\right) \end{aligned} \quad (2.30)$$

From this, the velocity of the first p-vortex can be derived as

$$\begin{aligned} -u_{1p\xi} + i v_{1p\eta} &= \left[dw_{1p}(\zeta)/d\zeta \right]_{\zeta=\zeta_{1p}} \\ &= -U e^{-i\alpha} + \frac{U c^2}{\zeta_{1p}^2} e^{i\alpha} - i \frac{\Gamma_{1p}}{2\pi} \frac{1}{\left(\zeta_{1p} - c^2/\bar{\zeta}_{1p}\right)} \\ &\quad - i \frac{\Gamma_{1q}}{2\pi} \frac{1}{\left(\zeta_{1p} - \zeta_{1q}\right)} + i \frac{\Gamma_{1q}}{2\pi} \frac{1}{\left(\zeta_{1p} - c^2/\bar{\zeta}_{1q}\right)} \end{aligned}$$

Solving the right-hand side of this equation, the real part gives the ξ -component and imaginary the η -component of velocity of Γ_{1p}

In the physical plane

$$(-u_{1p_x} + i v_{1p_y}) = (-u_{1p_\xi} + i v_{1p_\eta}) \frac{\zeta_{1p}^2}{\zeta_{1p}^2 - c^2} - i \frac{\Gamma_{1p}}{2\pi} \frac{\zeta_{1p} c^2}{(\zeta_{1p}^2 - c^2)^2} \quad (2.32)$$

Similarly,

$$\begin{aligned} w_{1q}(\zeta) &= w(\zeta) + i \frac{\Gamma_{1q}}{2\pi} \ln(\zeta - \zeta_{1q}) \\ &= -U \left(\zeta e^{-i\alpha} + \frac{c^2}{\zeta} e^{i\alpha} \right) - i \frac{\Gamma_{1p}}{2\pi} \ln\left(\zeta - \frac{c^2}{\bar{\zeta}_{1p}}\right) \\ &\quad + i \frac{\Gamma_{1p}}{2\pi} \ln(\zeta - \zeta_{1p}) + i \frac{\Gamma_{1q}}{2\pi} \ln\left(\zeta - \frac{c^2}{\bar{\zeta}_{1q}}\right) \end{aligned} \quad (2.33)$$

$$\begin{aligned} -u_{1q_\xi} + i v_{1q_\eta} &= [dw_{1q}(\zeta)/d\zeta]_{\zeta=\zeta_{1q}} \\ &= -U e^{-i\alpha} + \frac{U c^2}{\zeta_{1q}^2} e^{i\alpha} - i \frac{\Gamma_{1p}}{2\pi} \frac{1}{(\zeta_{1q} - c^2/\bar{\zeta}_{1p})} \\ &\quad + i \frac{\Gamma_{1p}}{2\pi} \frac{1}{(\zeta_{1q} - \zeta_{1p})} + i \frac{\Gamma_{1q}}{2\pi} \frac{1}{(\zeta_{1q} - c^2/\bar{\zeta}_{1q})} \end{aligned} \quad (2.34)$$

$$(-u_{1q_x} + i v_{1q_y}) = (-u_{1q_\xi} + i v_{1q_\eta}) \frac{\zeta_{1q}^2}{\zeta_{1q}^2 - c^2} + i \frac{\Gamma_{1q}}{2\pi} \frac{\zeta_{1q} c^2}{(\zeta_{1q}^2 - c^2)^2} \quad (2.35)$$

Thus, after these calculations, we know the positions and velocities of the first vortices introduced into the flow

After introducing Γ_{1p} and Γ_{1q} , we introduce two nascent vortices $\Delta\Gamma_{op}$ and $\Delta\Gamma_{oq}$ each of strength equal to Δt in accordance with Equation 2.25

First vortices are then convected in physical plane for a time interval of Δt in five steps of $\frac{1}{5} \Delta t$ using the expressions

$$x(t + \frac{1}{5} \Delta t) = x(t) + \frac{1}{5} u(t) \Delta t \quad (2.36)$$

$$y(t + \frac{1}{5} \Delta t) = y(t) + \frac{1}{5} v(t) \Delta t \quad (2.37)$$

After the time step Δt , we again add $\Delta\Gamma_{op} = \Delta\Gamma_{oq} = \Delta t$. This procedure is repeated five times till the first vortices are convected for $5\Delta t$. The velocities of Γ_1 and Γ_o vortices are computed after every time interval Δt , and thus the updated velocities are used for convection.

At time $5\Delta t$, the last nascent vortices are renamed as first vortices and the first vortices are renamed as second. We repeat the above procedure of introduction and convection four times in order to have four vortices in each shear layer.

Having introduced four vortices of constant strength we can now introduce new vortices of strengths calculated using the velocities U_{sh_p} and U_{sh_q} defined earlier and given by Equations 2.22 and 2.23. Thus,

$$\Delta\Gamma_{op} = \frac{1}{2} U_{sh_p}^2 \Delta t \quad (2.38)$$

$$\Delta\Gamma_{oq} = \frac{1}{2} U_{sh_q}^2 \Delta t \quad (2.39)$$

Positions ζ_{op} and ζ_{oq} of the nascent vortices Γ_{op} and Γ_{oq} are then calculated using the Kutta condition equations.

We then convect the first vortices in 5 steps of $\frac{1}{5} \Delta t$ and

also calculate their velocities prior to each step

The velocities of rest of the vortices are then calculated and these vortices are convected in a single step of Δt

We repeat the above steps 5 times so as to convect all the vortices for $5\Delta t$

At this stage, the vortices are renamed and new nascent vortices are introduced into the flow

This way we evolve the wake behind a flat plate for any time period by introducing the vortices accordingly

2.3.3 Removal and Coalescence of Vortices

The vortices which are very close to the plate induce very large velocities and lead to absurd results Sarpkaya(1975) has argued that vortices which approach the plate will tend to dissipate because of viscous action close to plate and, therefore, it might be prudent to remove such vortices A scheme has been used wherein any vortex that comes within $0.1c$ (2.5% of the plate length) is removed from calculation

Kiya and Arie(1980) have also discussed this problem According to them, it is probable that individual vortices come too close to the rear face of the plate and this causes them to have unreasonably high velocities along the plate owing to the presence of the image vortices within the circle in the transformed plane He, therefore, also removed the vortices in his model whenever they came nearer to the rear face of the plate than a specified distance

It has been well recognized that the orbiting motion of point vortices can rapidly affect neighboring vortices and that the

vortices of opposite circulation could remove themselves from the wake at high speeds when in close proximity. This is avoided by coalescing the vortices. Two vortices having same sign (i.e. positive or negative) are coalesced into a single vortex of the strength equal to the sum of the two whenever they come closer to each other than a distance equal to $0.1c$. In a similar manner two vortices of opposite sign also are removed from calculation whenever they come closer than $0.1c$ to each other. The distance $0.1c$ has been selected from the observation of Schaefer and Eskinazi (1959) who reported that a line vortex which has been in the wake of a viscous flow with a Reynolds number of about 40,000 for a period $t=8c/U$ will have a core radius of approximately $0.07c$. Thus the distance $0.1c$ is of the order of the core radius of a decaying vortex.

By the above methods, quite a large number of vortices are removed and the number of vortices to be handled decreases saving a lot of computer time.

RESULTS AND DISCUSSION

The computer code for the present work has been made in FORTRAN 77 language and run with the desired input parameters on the Convex 220 system

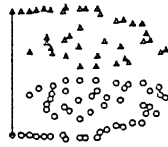
Numerical experiments were done to evolve the wake of a flat plate immersed in a uniform flow. Keeping in mind the availability of computer time, computations were made for only three cases as far as the angle of attack is concerned, viz. for flow normal to the plate, inclined at 85° to the plate and at 60° to the plate. To start with, the time-step Δt of 0.04 was selected for convection of vortices following Sarpkaya(1975) who on the basis of a number of numerical experiments with various values of Δt has concluded that this is the optimum time-step compromising between the computer time and the accuracy of results. The computations were done, however, with one more value of Δt , i.e., 0.03.

The results for all the cases studied are summarized below.

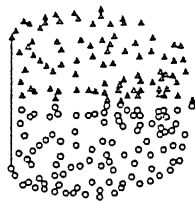
3.1 Case I. Plate Normal to the Flow

3.1.1 Time-step $\Delta t = 0.04$

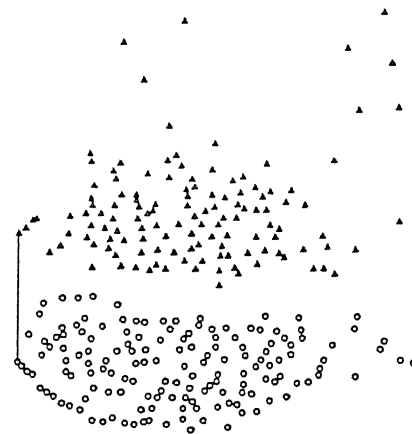
The program was run for $t = 180$. The results plotted in Figure 6 for various intermediate values of time starting from $t = 10$ show the step-by-step evolution of the wake. From the figure, it can be seen that the vortices start shedding symmetrically from



(a)

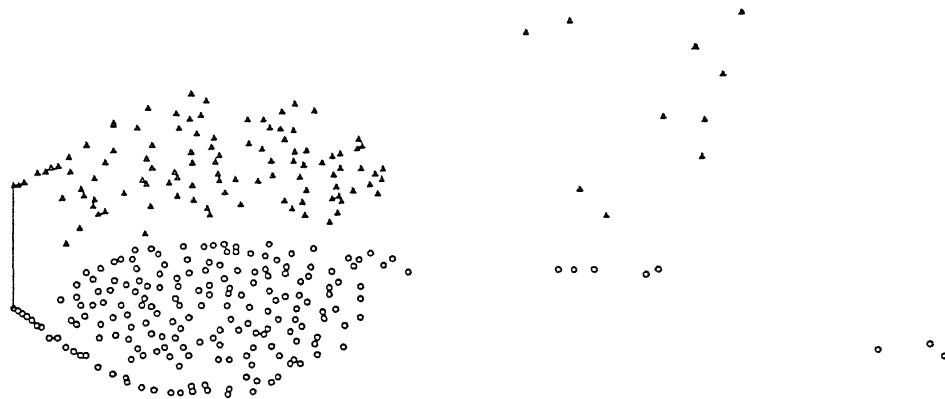


(b)

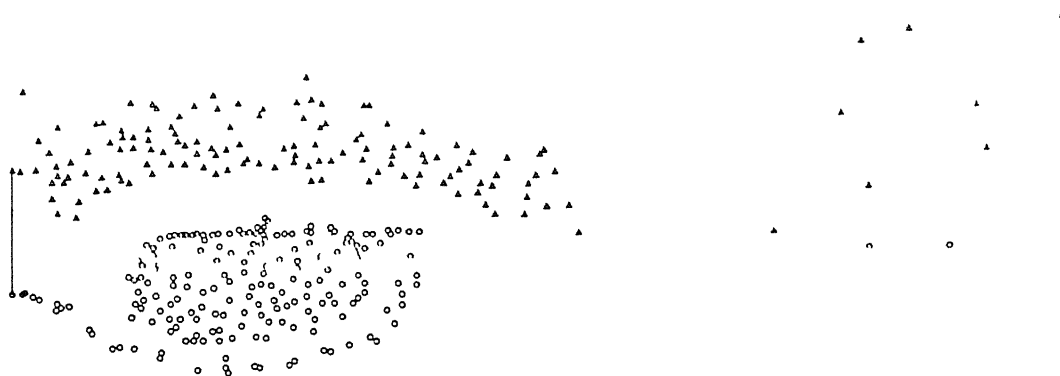


(c)

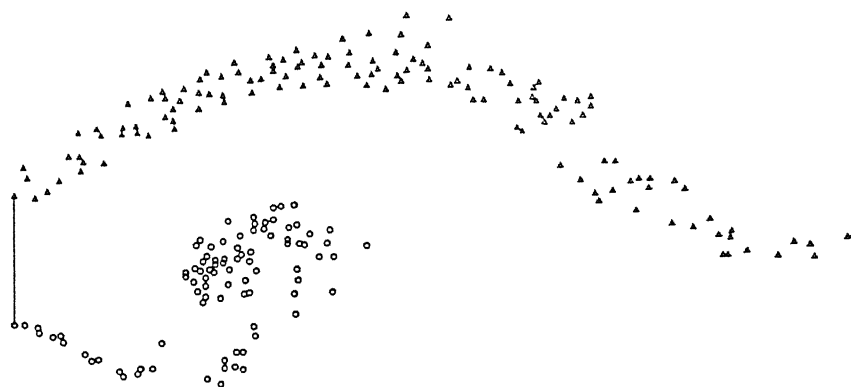
Figure 6 Evolution of wake behind a flat plate $\alpha = 90^\circ$, $\Delta t = 0.04$ (a) $t = 10$, (b) $t = 20$, (c) $t = 40$



(d)



(e)



(f)

Figure 6 Evolution of wake behind a flat plate $\alpha = 90^\circ$, $\Delta t = 0.04$ (contd) (d) $t = 50$, (e) $t = 60$, (f) $t = 70$



(g)



(h)



(i)

Figure 6 Evolution of wake behind a flat plate $\alpha = 90^\circ$, Δ 0 04 (contd) (g) $t = 80$, (h) $t = 90$, (i) $t = 100$

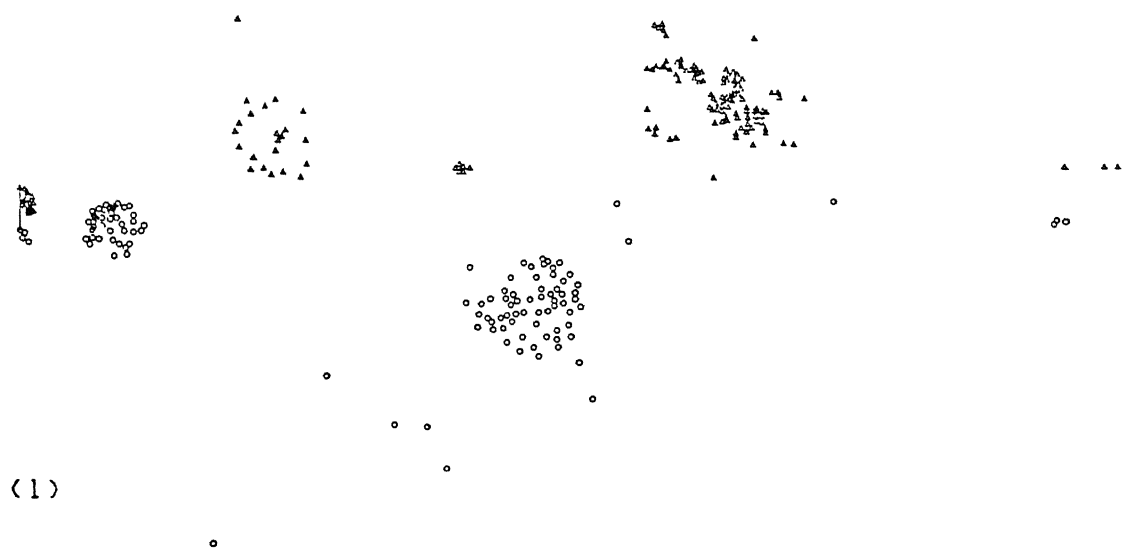
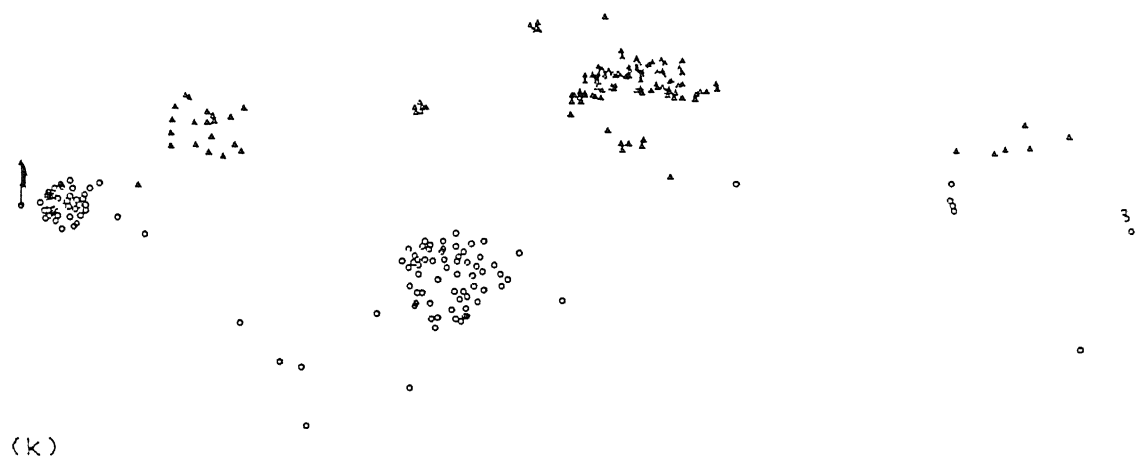
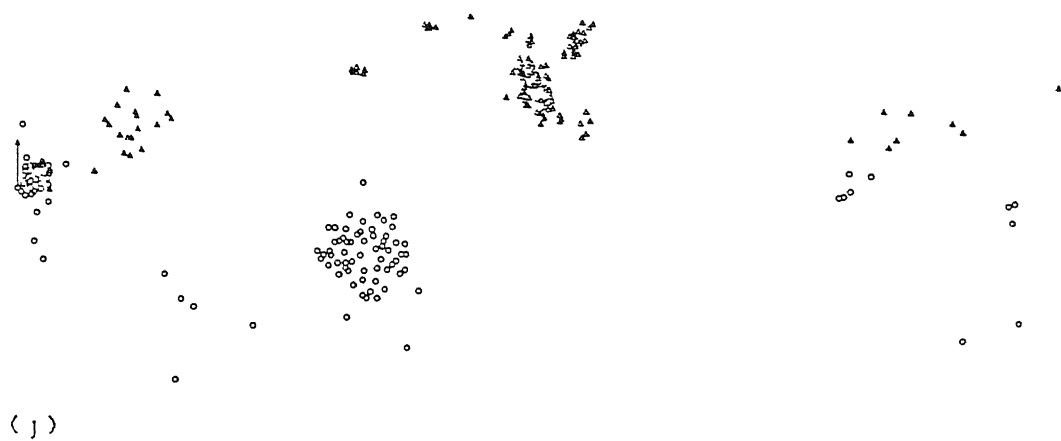
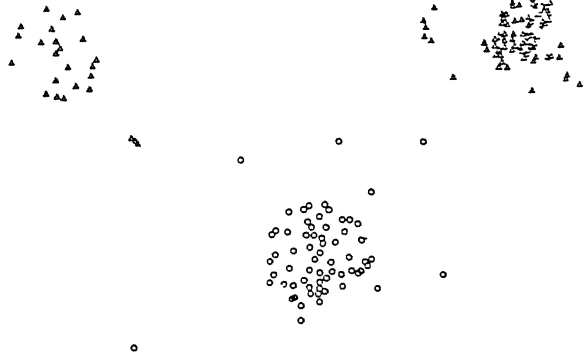


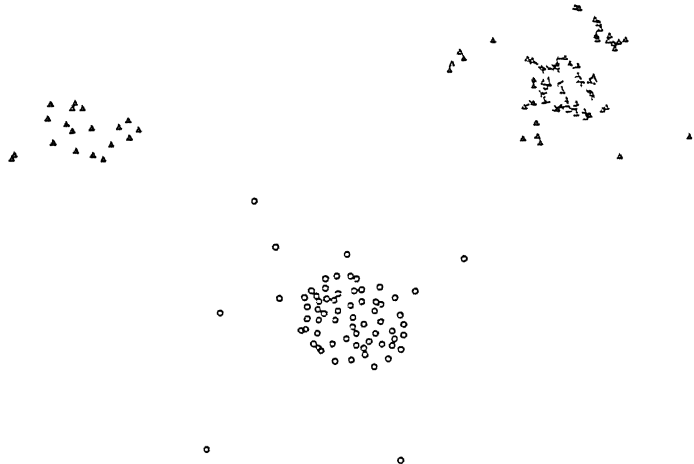
Figure 6 Evolution of wake behind a flat plate $\alpha = 90^\circ$, $\Delta t = 0.04$ (contd) (j) $t = 110$, (k) $t = 120$, (l) $t = 130$



(m)



(n)



(o)

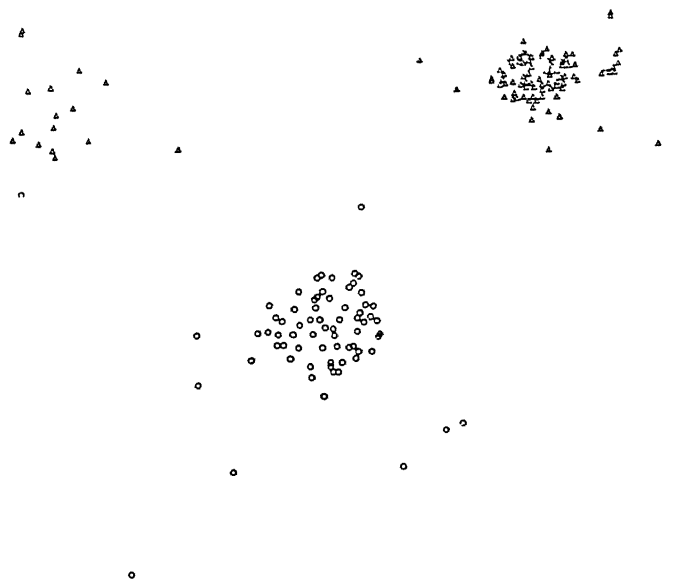


Figure 6 Evolution of wake behind a flat plate $\alpha = 90^\circ$, $\Delta t = 0.04$ (contd) (m) $t = 140$, (n) $t = 150$, (o) $t = 160$

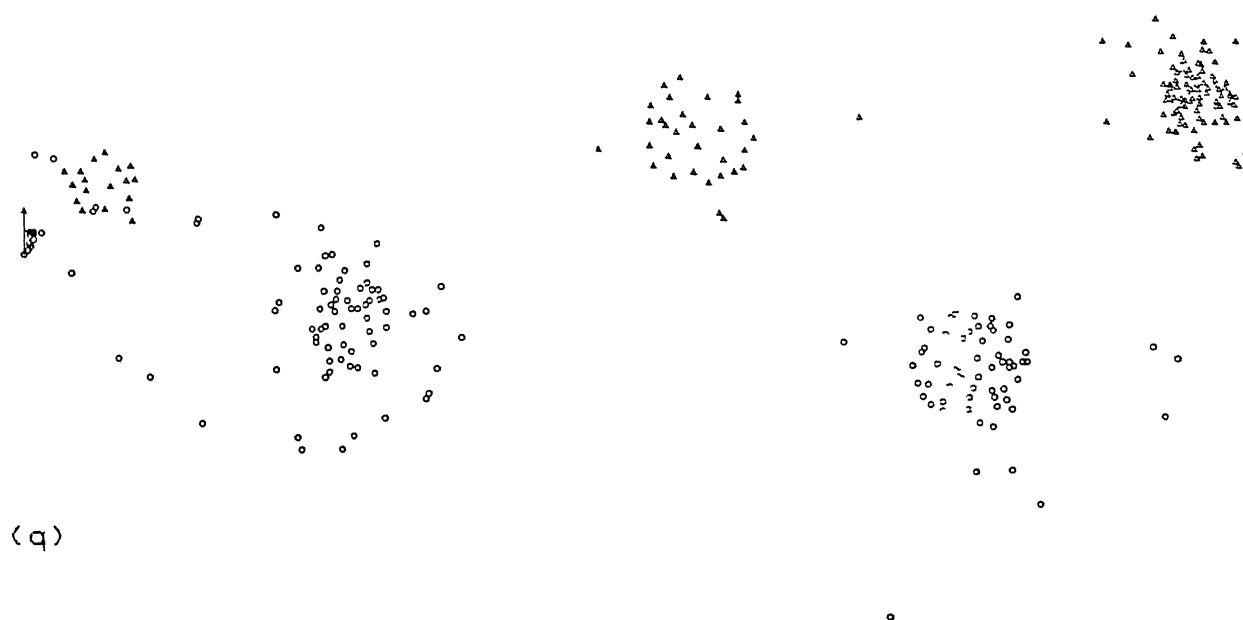


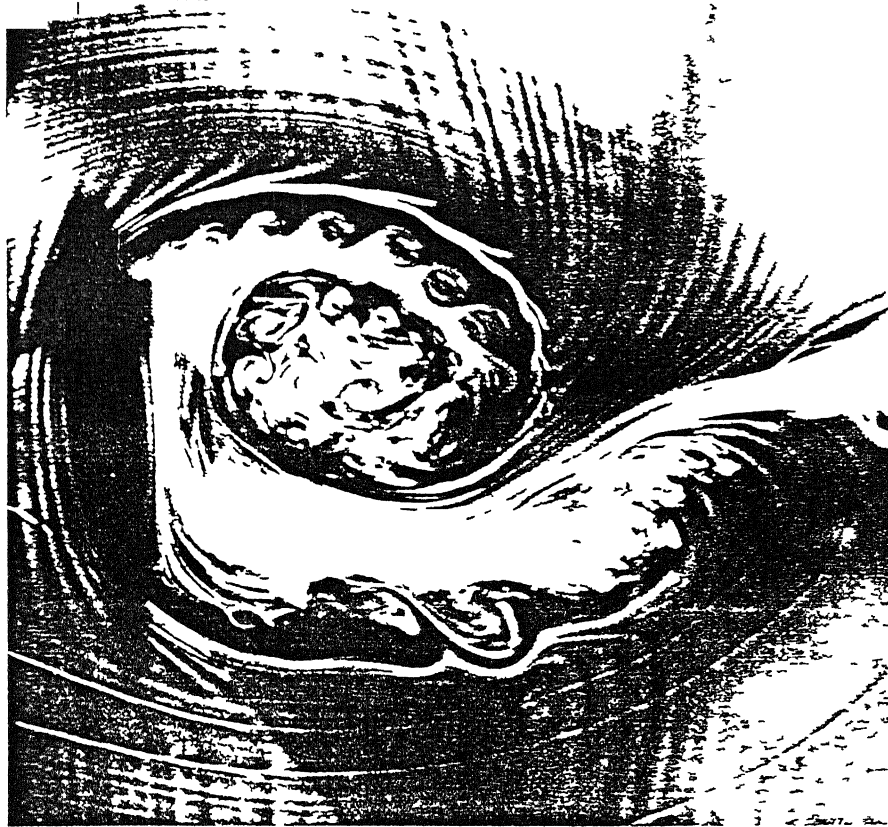
Figure 6 Evolution of wake behind a flat plate $\alpha = 90^\circ$, $\Delta t = 0.04$ (contd) (p) $t = 170$, (q) $t = 180$

both the edges of the plate and curve inwards in a very well defined manner. This type of symmetric pattern, however, does not last for long, and after $t = 20$, the asymmetry grows and a phase difference starts building up between the p- and q- vortex clusters. At $t = 70$, the picture clearly resembles the uniformly accelerated flow picture around an airfoil at 80° angle of attack (Figure 7). At around $t = 80$, vortex clouds start shedding from both the edges of the plate. The majority of the vortices congregate in clouds and move with the clouds as a whole. At the later time, the distribution of these vortex clusters clearly resembles the von Karman vortex street. The availability of computer time put a constraint on running the program further. The computer time taken by the run was 8 hours.

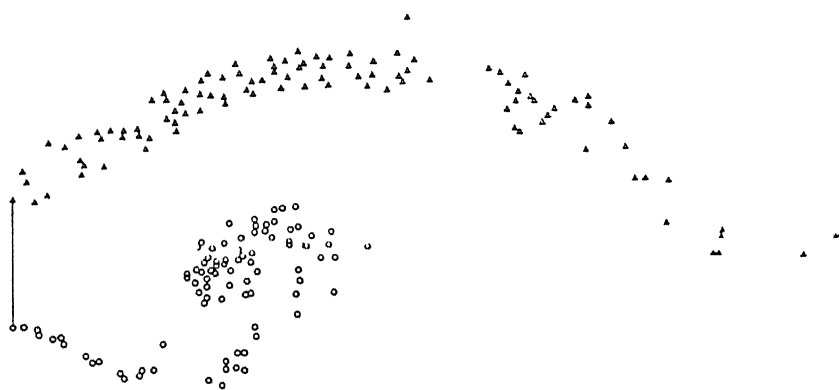
The flow pattern thus clearly exhibits the following major features as also noted by other investigators:

- 1) The wake starts developing symmetrically and it is only after some time that the asymmetry sets in. Unlike the work of Sarpkaya and Shoaff (1979), who used artificial perturbation method to induce asymmetry while modelling the flow over a circular cylinder, in the present computation, the flow became asymmetric by its own. It is felt that the rounding errors probably have caused slight asymmetry, which once set in, grows with time.

In this context, it is appropriate to report the work of Kiya and Arie (1980) who inclined the flat plate by 5° from the normal position to avoid the introduction of artificial asymmetry of flow to initiate the periodic vortex shedding.



(a)



(b)

Figure 7 Start of asymmetry of wake
 a) uniformly accelerated flow around an airfoil at 80° angle of attack (Reproduced from American Scientist, Vol 72, 1984),
 b) wake flow pattern behind the flat plate during the early stage of flow development computed in the present study

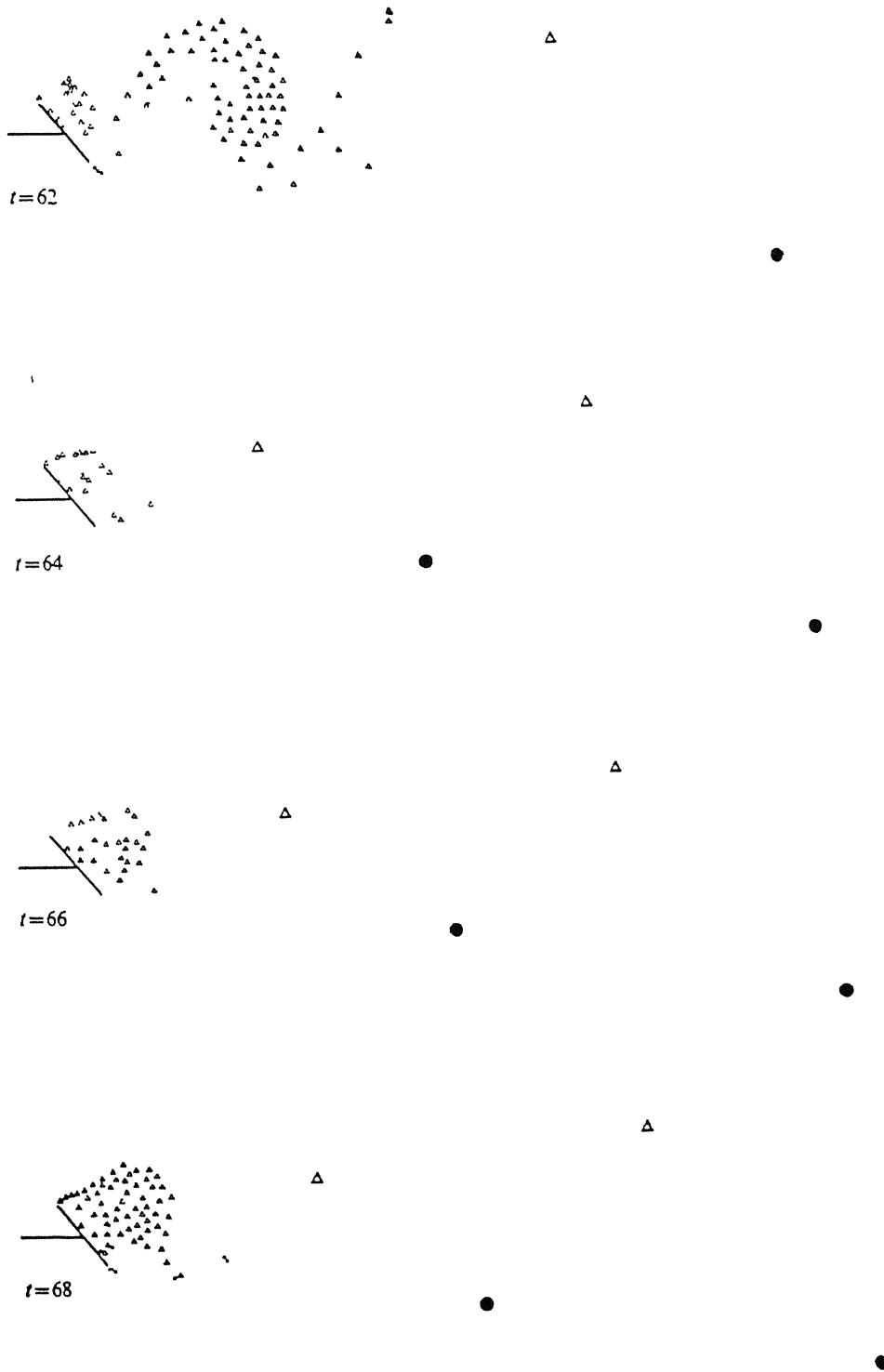


Figure 8 Vortex arrangements behind a flat plate $\alpha = 50^\circ$
(Sarpkaya, 1975)

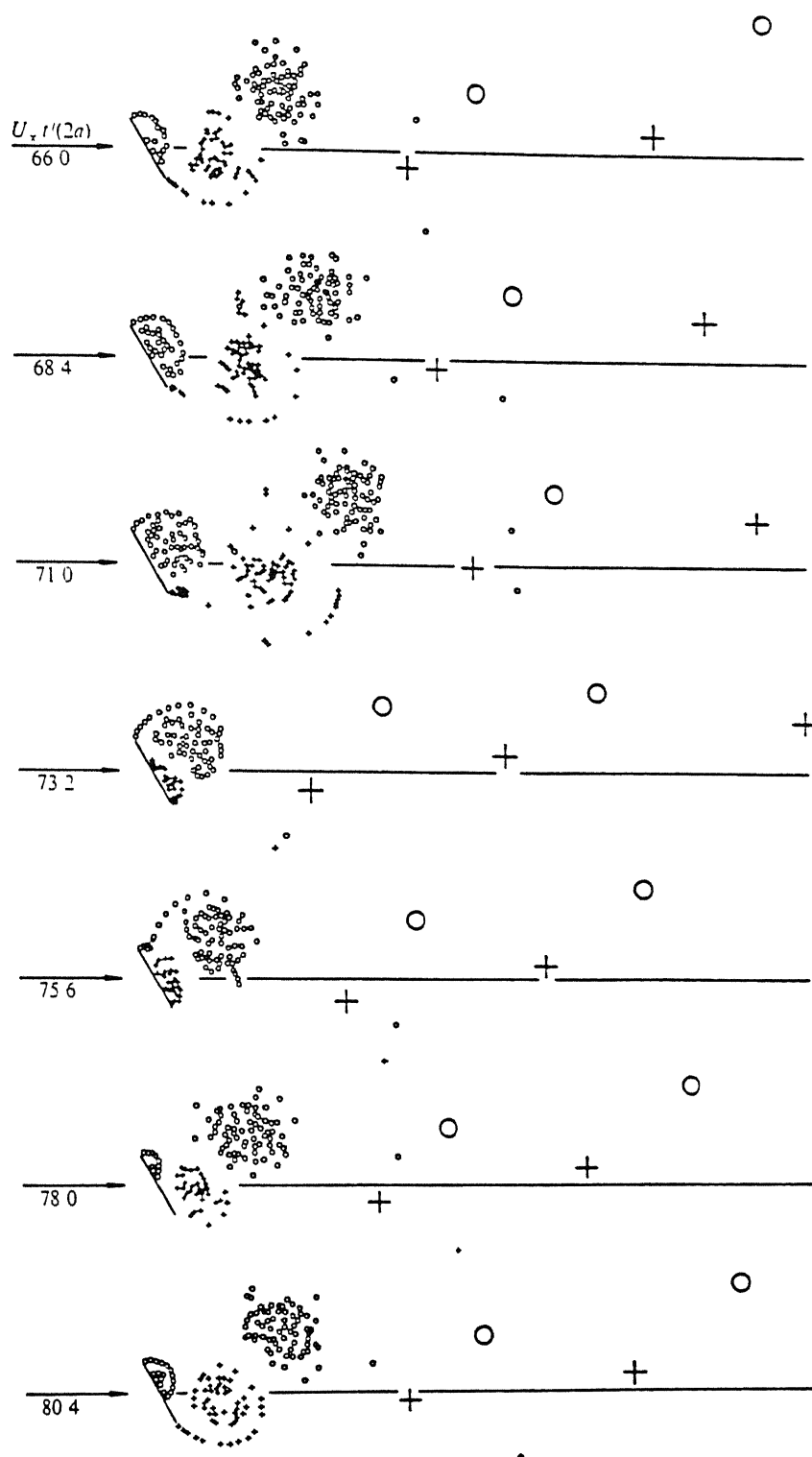


Figure 9 Vortex pattern behind a flat plate $\alpha = 60^\circ$ (Kiyama and Arie, 1977)

11) Once the asymmetry sets in, the pattern of vortex shedding is established and we can make an estimate of Strouhal number

$$St = f L/U$$

where f is the frequency of vortex shedding

In this phase of regular vortex shedding, the frequency is estimated as about 1 in 25 seconds giving a value of St as 0.16. This compares favorably with the experimental results of Abernathy(1962) who obtained $St = 0.164$ in the range of $40^\circ < \alpha < 80^\circ$ and the calculated results of Sarpkaya(1975) for the same range and Kiya and Arie(1977) (Figures 8 and 9) who calculated the value of St as 0.154 and 0.14 respectively

3.1.2 Time-step $\Delta t = 0.03$

The program with $\Delta t = 0.03$ could be run for $t = 130$. In this case also the flow started symmetrically but became asymmetric at a later stage (Figure 10). This time, the periodic vortex shedding started at time $t = 60$, which is lesser than with $\Delta t = 0.04$. This is justified considering the fact that the rounding off errors are introduced faster with smaller value of time-step.

The vortex shedding frequency, however, in this case was $1/15$ as against $1/25$ for $\Delta t = 0.04$, giving $St = 0.26$, which is much higher than the expected result.

3.2 Plate inclined at 85° to the Flow

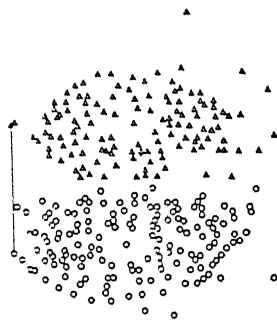
For $\alpha = 85^\circ$, the program was run with $\Delta t = 0.04$ only and for a time $t = 70$. The results for $\alpha = 85^\circ$ are plotted in Figure 11. The asymmetry, in this case starts right from the beginning and



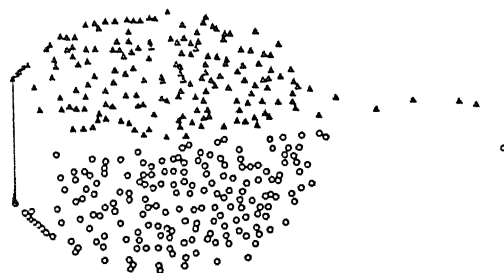
(a)



(b)

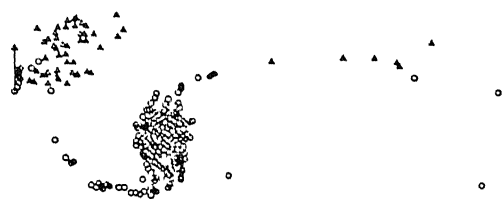


(c)

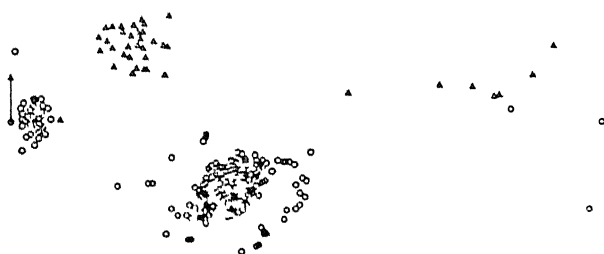


(d)

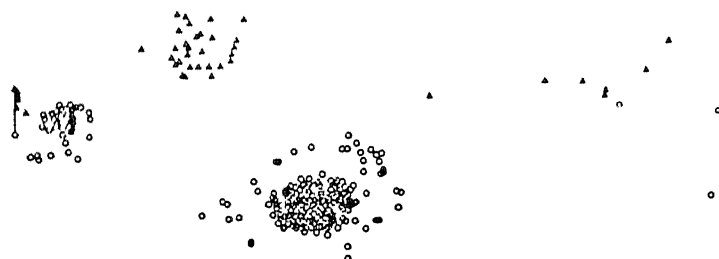
Figure 10 Evolution of wake behind a flat plate $\alpha = 90^\circ$, $\Delta t = 0.03$ (a) $t = 10$, (b) $t = 20$, (c) $t = 30$, (d) $t = 40$



(e)



(f)



(g)

Figure 10 Evolution of wake behind a flat plate $\alpha = 90^\circ$, $\Delta t = 0.03$ (contd) (e) $t = 60$, (f) $t = 70$, (g) $t = 80$

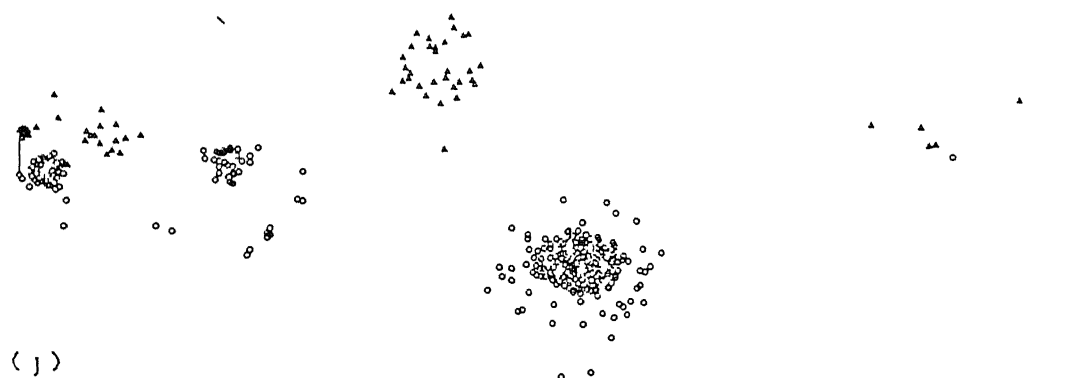
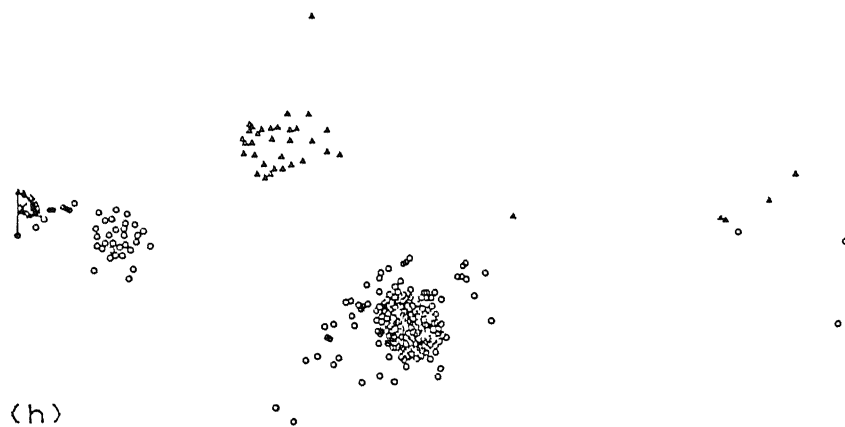


Figure 10 Evolution of wake behind a flat plate $\alpha = 90^\circ$, $\Delta t = 0.03$ (contd) (h) $t = 90$, (i) $t = 100$, (j) $t = 110$

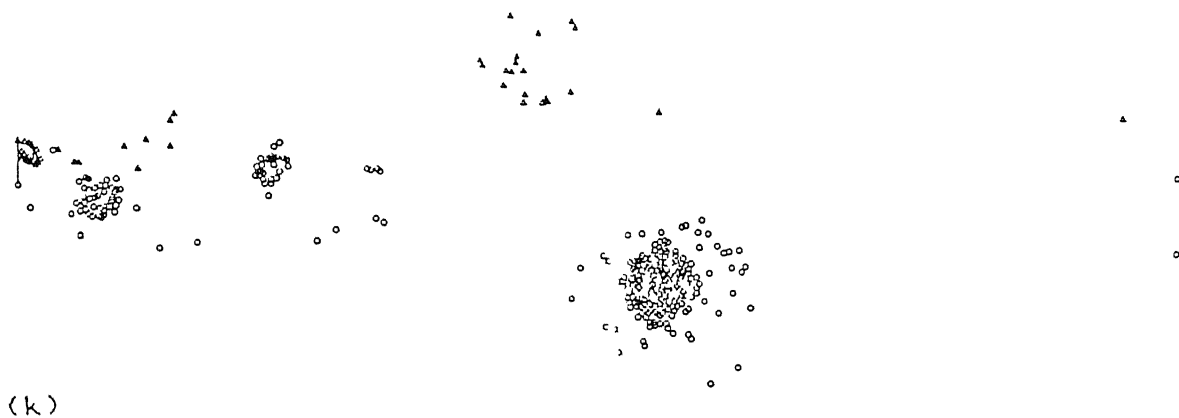


Figure 10 Evolution of wake behind a flat plate $\alpha = 90^\circ$, $\Delta t = 0.03$ (contd) (k) $t = 120$, (l) $t = 130$



Figure 11 Vortex shedding pattern behind an inclined flat plate $\alpha = 85^\circ$, $\Delta t = 0.04$ (a) $t = 10$, (b) $t = 20$, (c) $t = 30$, (d) $t = 40$

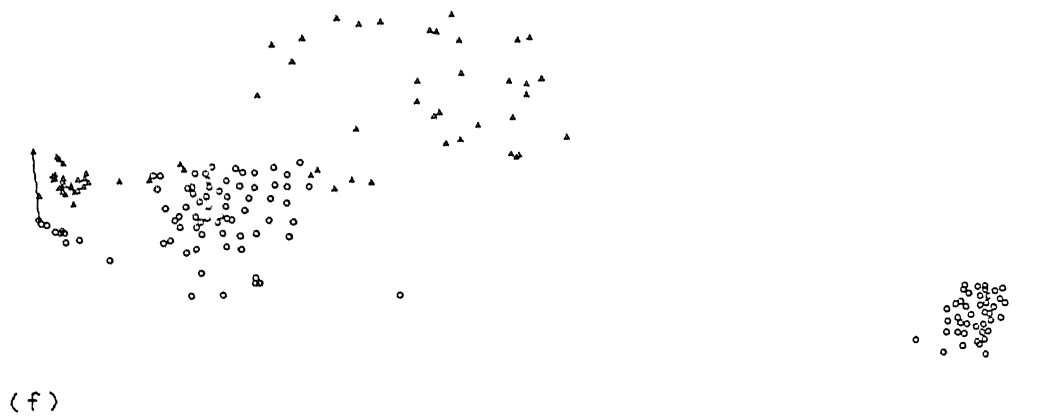
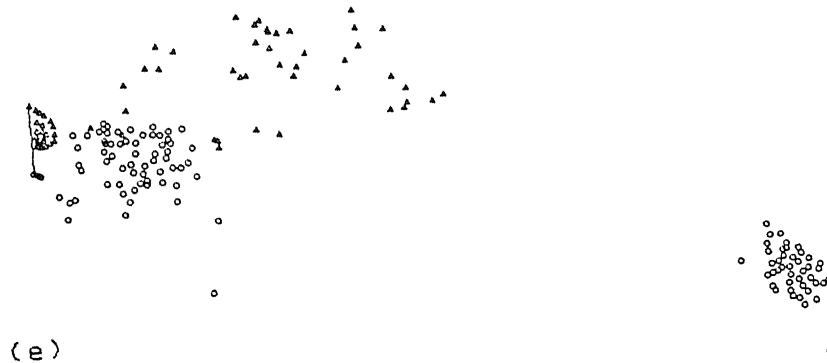


Figure 11 Vortex shedding pattern behind an inclined flat plate
 $\alpha = 85^\circ$, $\Delta t = 0.04$ (contd) (e) $t = 50$, (f) $t = 60$, (g) $t = 70$

vortex clouds shed alternately. It was however, difficult to find out the Strouhal number in this case from the vortex shedding pattern as the frequency of shedding could not be established from data output.

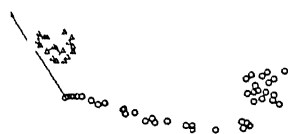
3.3 Plate Inclined at 60° to the Flow

The vortices in this case start shedding asymmetrically as expected. The picture, however, was noticeably different from the other cases described earlier. Here, the p- vortices which are shed from the trailing edge at the start of the flow leave the edge and convect downstream and for a long time the other p- vortex cloud is not formed. The q- vortex cluster on the leading edge grows in size during this period. It is only at $t = 170$ that the second p- vortex cloud starts forming. At $t = 180$ the clouds leave the plate and shed with a phase difference as can be seen from Figure 12.

This type of delayed vortex shedding, however, is not considered to be due to any error in the code as Kiya and Arie(1977) have also reported that the periodic flow patterns cannot be predicted from vortex patterns in an early stage of the flow development.

As the program could not be run beyond this time, the flow features could not be studied fully and the Strouhal number could not be estimated.

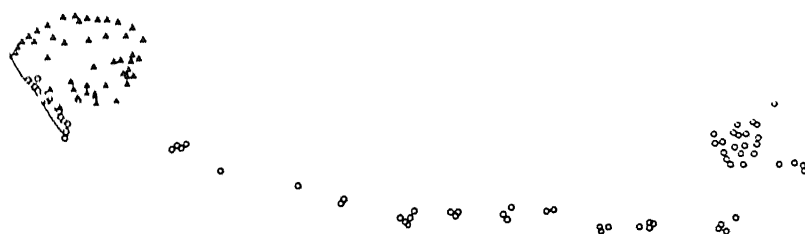
It was tried to compute the results for this angle of attack with a time step of 0.03 also. The program, however, could not be run for a longer time. The results for $t = 10$ to 40 are plotted in Figure 13.



(a)



(b)



(c)

Figure 12 Vortex pattern behind an inclined flat plate $\alpha = 60^\circ$,
 $\Delta t = 0.04$ (a) $t = 10$, (b) $t = 20$, (c) $t = 30$

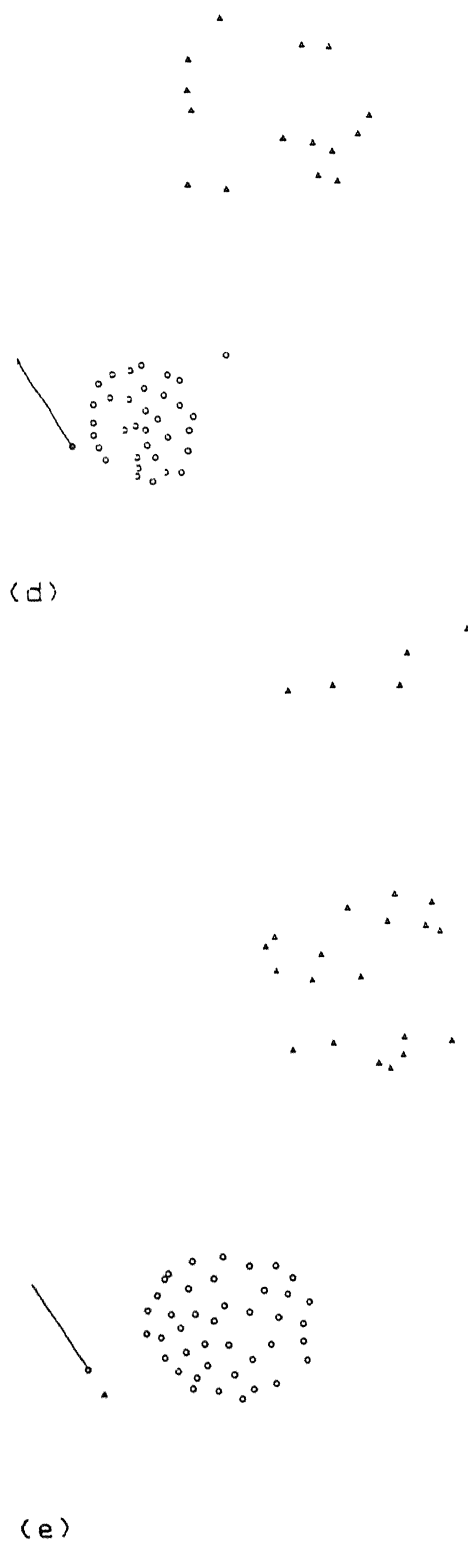


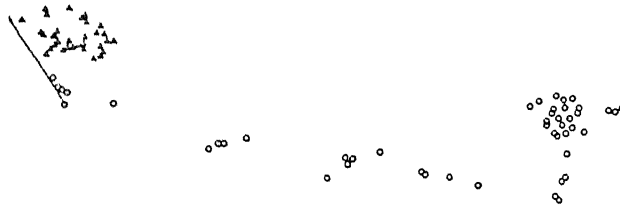
Figure 12 Vortex pattern behind an inclined flat plate $\alpha = 60^\circ$, $\Delta t = 0.04$ (contd) (d) $t = 180$, (e) $t = 190$



(a)



(b)



(c)



(d)

Figure 13 Vortex pattern behind an inclined flat plate $\alpha = 60^\circ$, $\Delta t = 0.03$ (a) $t = 10$, (b) $t = 20$, (c) $t = 30$, (d) $t = 40$

On analyzing the data for various cases studied it is felt that probably a little more attention has to be paid to study the way the nascent vortices are introduced and the Kutta condition

CONCLUSIONS

In the present work the vortex shedding behind a flat plate has been numerically studied using the discrete vortex method, in which the shear layers which emanate from the leading and trailing edges of the plate are represented by an array of discrete vortices through the use of the complex potential and the conformal transformation between the plate and the circle plane. Kutta condition has been used to determine the locations of the nascent vortices. The model which is a simpler implementation than the other reported methods reproduces the results that have been reported. The onset of asymmetry occur earlier in our procedure, probably because of the approximation involved in the application of Kutta condition.

The Strouhal numbers predicted are around the same values as reported earlier.

This implementation has not been able to calculate satisfactorily the flows for small values of angle of attack wherein the chaos sets in before recognizable vortex clusters are developed. This may be because of rather severe dissipation of vortices in the rear-face shear layer modelled here.

It is felt that to save building up of truncation errors, and incidentally to save time for calculations, the vortex clusters once they are identifiable should be replaced by a coalesced

single vortex Sarpkaya(1975) and Kiya and Arie(1977) have implemented such schemes with benefit. The scheme could not be implemented in the present study due to lack of time.

Another apparently useful approach to try is to combine the vortex cloud method with the cloud-in-cell method. None of the reported work has handled the separation phenomena by cloud-in-cell method. One could use the vortex cloud method for the formation of the nascent vortices, but once the vortices are formed, the convection can possibly be handled by the cloud-in-cell procedure.

REFERENCES

- ABERNATHY, F H , 1962, Flow Over an Inclined Plate *J Basic Engg , Trans A S M E* , Vol D 84, pp 380
- ABERNATHY F H and KRONAUER, R E , 1962, The Formation of Vortex Streets, *J Fluid Mech* , Vol 13, pp 1-20
- BAKER, G R , 1979, The Cloud in Cell Technique Applied to the Roll-up of Vortex Sheets, *J Comput Phys* , Vol 31, pp 76-95
- BIRDSALL C K , and FUSS, D , 1969 Clouds-in-Clouds, Clouds-in-Cells Physics for Many-Body Plasma Simulation, *J Comput Phys* , Vol 3, pp 494-511
- CHRISTIANSEN, J P , 1973, Numerical Simulation of Hydrodynamics by the Method of Point Vortices, *J Comput Phys* , Vol 13, pp 363-379
- CLEMENTS, R R , 1973, An Inviscid Model of Two-Dimensional Vortex Shedding, *J Fluid Mech* , Vol 57, pp 321-336
- CLEMENTS R R , and MAULL, D J , 1975, The Representation of Sheets of Vorticity by Discrete Vortices, *Prog Aerospace Sci* , Vol 16, pp 129-146
- FAGE, A , and JOHANSEN, F C , 1928 The Structure of Vortex Sheets, *Phil Mag* , Series 7, Vol 5, pp 417-441
- HARLOW, F H , 1964, The Particle-in-Cell Computing Methods for Fluid Dynamics, *Methods in Computational Phys* , (Eds B Adler et al), Vol 3, pp 319-343, Academic Press
- KIYA, M , and ARIE, M , 1977, A Contribution to an Inviscid Vortex-Shedding Model for an Inclined Flat Plate in Uniform Flow, *J Fluid Mech* , Vol 82, pp 223-240
- KIYA, M , and ARIE, M , 1980, Discrete Vortex Simulation of Unsteady Separated Flow Behind a Nearly Normal Plate, *Bulletin of JSME*, Vol 23, No 183, pp 1451-1458
- LANGDON, A B , 1970, Effects of the Spatial Grid in Simulation Plasmas, *J Comput Phys* , Vol 6, pp 247-267
- MAIR, W A and MAULL, D J , 1971, Bluff Bodies and Vortex Shedding-A Report on Euromech 17, *J Fluid Mech* , Vol 45, pp 209
- MILNE-THOMSON, L M , 1969, *Theoretical Hydrodynamics*, 5th ed , The MacMillan Co , New York

- SAFFMAN, P G , and BAKER, G R , 1979, Vortex Interactions, *Ann Rev Fluid Mech* , Vol 11, pp 95-122
- SARPKAYA T , 1975, An Inviscid Model of Two-Dimensional Vortex Shedding for Transient and Asymptotically Steady Separated Flow over an Inclined Flat Plate, *J Fluid Mech* , Vol 68, pp 109-128
- SARPKAYA T , 1979, Vortex-Induced Oscillations - A Selective Review, *ASME J Applied Mech* , Vol 46, pp 241-258
- SARPKAYA T , 1989 Computational Methods with Vortices - The 1988 Freeman Scholar Lecture, *J Fluids Engg* , Transactions of the ASME, Vol 111, pp 5-52
- SARPKAYA, T , and SHOAFF, R L , 1979, An Inviscid Model of Two-Dimensional Vortex Shedding for Transient and Asymptotically Steady Separated Flow over a Cylinder, *AIAA J* , Vol 17, No 11 pp 1193-1200
- SARPKAYA, T , and KLINE, H K , 1982, Impulsively-Started Flow About Four Types of Bluff Bodies, *ASME J Fluids Engg* , Vol 104, No 2, pp 207-213
- SARPKAYA, T , and IHRIG, C J , 1986, Impulsively Started Flow About Rectangular Prisms Experiments and Discrete Vortex Analysis, *ASME J Fluids Engg* , Vol 108, pp 47-54
- SARPKAYA, T , MOSTAFA, S M , and MUNZ P D , 1990, Numerical Simulation of Unsteady Flow About Cambered Plates, *J Aircraft*, Vol 27, No 1, pp 51-59
- SCHAEFER, J W , and ESKINAZI, S , 1959 An Analysis of the Vortex Street Generated in a Viscous Fluid, *J Fluid Mech* , Vol 6, pp 241
- SMITH, P A and STANSBY, P K , 1987, Generalized Discrete Vortex Method for Cylinders Without Sharp Edges, *AIAA J* , Vol 25, No 2, pp 199-200

AE-1993-M-KUM-DIS